

RESEARCH ARTICLE

Retrotransposon derepression leads to activation of the unfolded protein response and apoptosis in pro-B cells

Alessandra Pasquarella¹, Anja Ebert^{2,*}, Gustavo Pereira de Almeida^{1,*}, Maria Hinterberger³, Maryam Kazerani¹, Alexander Nuber¹, Joachim Ellwart⁴, Ludger Klein³, Meinrad Busslinger² and Gunnar Schotta^{1,†}

ABSTRACT

The H3K9me3-specific histone methyltransferase *Setdb1* impacts on transcriptional regulation by repressing both developmental genes and retrotransposons. How impaired retrotransposon silencing may lead to developmental phenotypes is currently unclear. Here, we show that loss of *Setdb1* in pro-B cells completely abrogates B cell development. In pro-B cells, *Setdb1* is dispensable for silencing of lineage-inappropriate developmental genes. Instead, we detect strong derepression of endogenous murine leukemia virus (MLV) copies. This activation coincides with an unusual change in chromatin structure, with only partial loss of H3K9me3 and unchanged DNA methylation, but strongly increased H3K4me3. Production of MLV proteins leads to activation of the unfolded protein response pathway and apoptosis. Thus, our data demonstrate that B cell development depends on the proper repression of retrotransposon sequences through *Setdb1*.

KEY WORDS: *Setdb1*, Heterochromatin, Retrotransposon, Unfolded protein response, Mouse

INTRODUCTION

Epigenetic mechanisms regulate developmental transitions by mediating the activation or stable repression of lineage-appropriate or lineage-inappropriate genes, respectively. Dysregulation of epigenetic machineries therefore has adverse consequences for development. In the context of hematopoiesis, impairment of repressive chromatin marks, such as DNA methylation, or Polycomb silencing result in compromised stem and progenitor cell differentiation and may even lead to the development of malignancies (Beguelin et al., 2013; Su et al., 2003). Another major repression mechanism involves the heterochromatin modification H3K9me3. This modification is broadly enriched at pericentric heterochromatin, various classes of retrotransposons, imprinted loci and repressed developmental genes. The histone methyltransferase *Setdb1* mainly controls H3K9me3 outside of pericentric heterochromatin and plays crucial roles in development (Karimi et al., 2011; Regha et al., 2007). *Setdb1* mutant embryos die even before implantation (Dodge

et al., 2004), and conditional inactivation of *Setdb1* during neurogenesis or in mesenchymal cells coincides with severe developmental phenotypes (Lawson et al., 2013; Tan et al., 2012; Yang et al., 2013). Thus, *Setdb1*-mediated H3K9me3 appears to regulate developmental transitions.

The functions of *Setdb1* have been well characterized in mouse embryonic stem cells (ESCs). In these cells, *Setdb1* depletion leads to the derepression of lineage-specifying genes and loss of pluripotency. Transcriptional dysregulation in *Setdb1*-deficient ESCs is due to the loss of H3K9me3 from promoter regions of lineage genes (Bilodeau et al., 2009; Yuan et al., 2009). In addition, *Setdb1*-deficient ESCs are characterized by enhanced transcription of retrotransposons. How retrotransposon derepression might have phenotypic consequences is unclear. Two hypotheses are currently discussed. First, that derepression of retrotransposons leads to elevated transcription of neighboring genes through enhancer action of chimeric transcripts (Karimi et al., 2011; Matsui et al., 2010). This, in turn, might impair the transcriptional stability in cells. Second, that enhanced activity of functional retrotransposon copies, which are still able to jump, may lead to mutations (Lee et al., 2012) or genomic instability (Bourc'his and Bestor, 2004).

Here, we show that conditional inactivation of *Setdb1* in pro-B cells leads to a block in B cell development. We found that *Setdb1*-deficient pro-B cells show derepression of specific classes of retrotransposons, among which the endogenous murine leukemia virus (MLV) elements exhibited the highest transcriptional activation. Notably, forced MLV expression coincides with massive production of MLV-derived proteins which, in turn, triggers activation of the unfolded protein response (UPR) and subsequent apoptosis of pro-B cells. Expression of pro-survival *Bcl2* antagonizes UPR-mediated apoptosis and leads to a partial rescue of B cell development, indicating that retrotransposon silencing is the primary role of *Setdb1* during early B cell development. In summary, our data provide a novel molecular explanation for the adverse consequences of impaired retrotransposon silencing during development.

RESULTS**Loss of *Setdb1* blocks B cell development**

Setdb1 is constitutively expressed during B cell development (Heng et al., 2008). To delete *Setdb1* specifically during early stages of B cell development, we generated a mouse strain in which we combined *Mb1* (*Cd79a*)-*Cre* with a conditional *Setdb1* allele that has the crucial exon 4 flanked by loxP sites. These *Mb1-Cre*; *Setdb1*^{lox/-} mice are referred to hereafter as *Setdb1*^{Mb1}, and *Mb1-Cre*; *Setdb1*^{lox/+} or +/+; *Setdb1*^{lox/+} mice provide the controls. *Mb1-Cre* initiates deletion of loxP-flanked regions at the transition from pre-pro-B cells to committed pro-B cells (Hobeika et al., 2006).

Spleen size was severely reduced in *Setdb1*^{Mb1} mice (Fig. 1A). Histological examination revealed reduced number and size of

¹Ludwig Maximilians University and Munich Center for Integrated Protein Science (CiPSM), Biomedical Center, 82152 Planegg-Martinsried, Germany. ²Research Institute of Molecular Pathology, Vienna Biocenter, 1030 Vienna, Austria. ³Ludwig Maximilians University, Institute for Immunology, 80336 München, Germany. ⁴Helmholtz Zentrum München, Institute of Molecular Immunology, 81377 München, Germany.

*These authors contributed equally to this work

†Author for correspondence (gunnar.schotta@med.uni-muenchen.de)

© G.S., 0000-0003-4940-6135

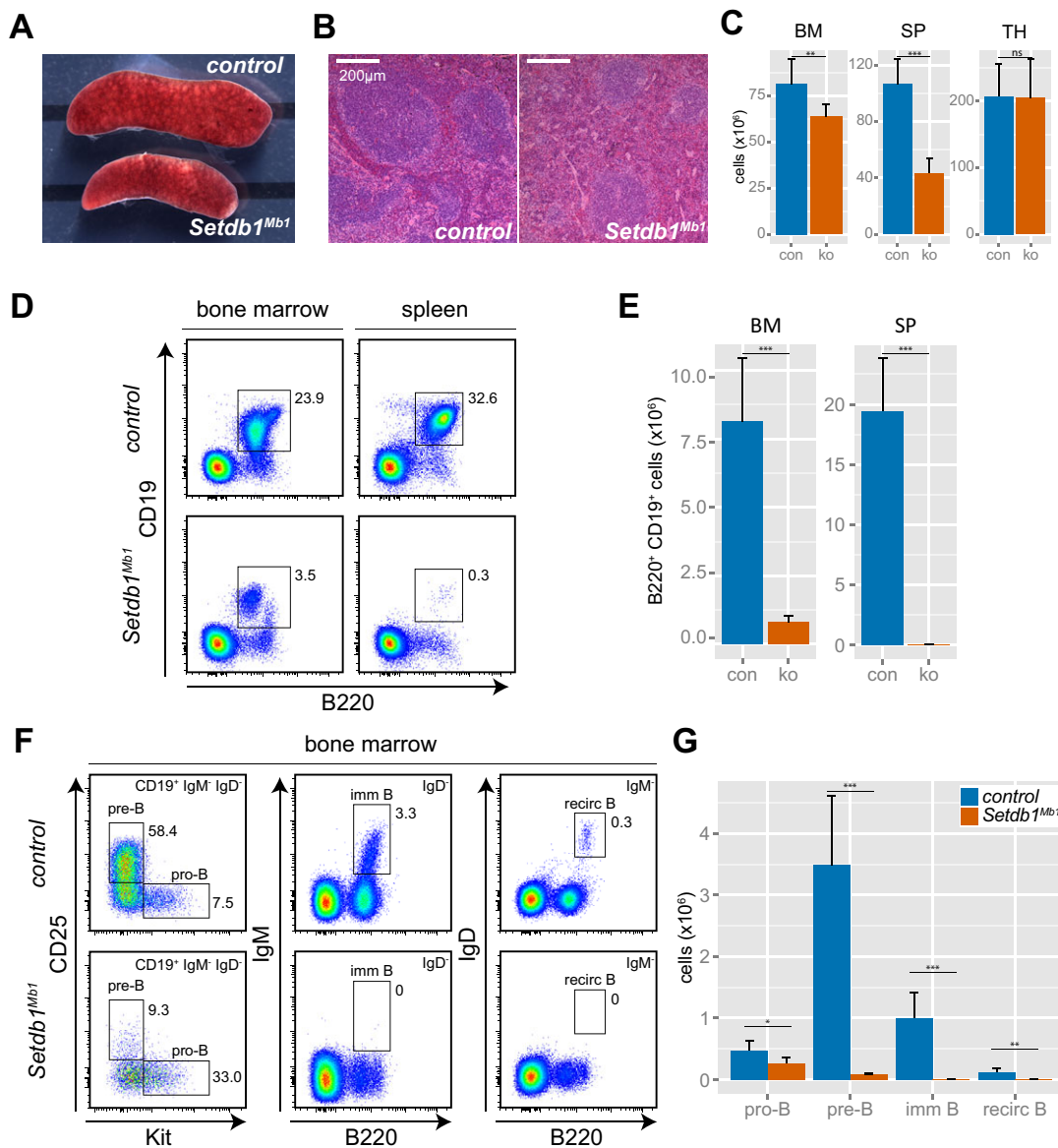


Fig. 1. Loss of *Setdb1* in early B cells leads to impaired B cell development. (A) Spleen of control (*Mb1-Cre; Setdb1^{flx/+}* or *+/+; Setdb1^{flx/+}*) and *Setdb1^{Mb1}* (*Mb1-Cre; Setdb1^{flx/-}*) mice. (B) Paraffin sections of control and *Setdb1^{Mb1}* spleen stained with Hematoxylin and Eosin. Areas with dark blue staining are follicles with accumulation of lymphocytes. (C) Total cell numbers of bone marrow (BM), spleen (SP) and thymus (TH) in control (con) and *Setdb1^{Mb1}* (ko) mice ($n=6$). (D) Representative FACS plots showing the B cell population (B220⁺ CD19⁺) in spleen and bone marrow of control and *Setdb1^{Mb1}* mice. (E) The average total numbers of B220⁺ CD19⁺ B cells in control and *Setdb1^{Mb1}* mice ($n=6$). (F) Representative FACS plots showing different stages of B cell development in the bone marrow of control and *Setdb1^{Mb1}* mice. (G) Average total cell numbers of B cell developmental stages in bone marrow from control and *Setdb1^{Mb1}* mice ($n=6$). (C,E,G) * $P<0.05$, ** $P<0.01$, *** $P<0.001$ (unpaired two-tailed Student's *t*-test); ns, not significant.

follicles (Fig. 1B). Total cell numbers of spleen and bone marrow were strongly reduced in *Setdb1^{Mb1}* mice (Fig. 1C). Consistent with the lack of *Mb1-Cre* activity in T cell development, no changes in thymus cell number were detected (Fig. 1C). FACS analysis of B cell markers revealed almost complete absence of B cells [B220 (Ptpcr)⁺ CD19⁺] in *Setdb1^{Mb1}* spleen and severely reduced B cell numbers in bone marrow (Fig. 1D,E). The lack of peripheral B cells prompted us to identify the stage at which B cell development is impaired in *Setdb1^{Mb1}* mice. Analysis of the B cell compartment in bone marrow revealed that the percentages of pro-B cells [CD19⁺ IgM⁻ IgD⁻ CD25 (Il2ra)⁻ Kit⁺] are comparable between control and *Setdb1^{Mb1}* mice; however, pre-B cells (CD19⁺ IgM⁻ IgD⁻ CD25⁺ Kit⁻) were severely reduced and neither immature (B220⁺ IgM⁺ IgD⁻) nor recirculating (B220⁺ IgM⁻ IgD⁺) B cells could be

detected (Fig. 1F,G). Analysis of hematopoietic stem cell and progenitor populations revealed no difference between control and *Setdb1^{Mb1}* mice, as expected (Fig. S1).

To test whether blocked B cell development was due to cell-intrinsic defects, we performed competitive transplantation experiments by injecting a 1:1 mixture of wild-type CD45.1 bone marrow progenitors together with control or *Setdb1^{Mb1}* bone marrow cells carrying the congenic marker CD45.2 into lethally irradiated recipients. Whereas the control bone marrow cells contributed to the B cell lineage comparably to the co-injected wild-type cells, *Setdb1^{Mb1}* B cells were hardly detectable in the periphery (Fig. 2A). Analysis of the B cell compartment in the bone marrow of transplanted mice revealed that *Setdb1^{Mb1}* B cells were severely compromised at the pre-B cell stage (Fig. S2).

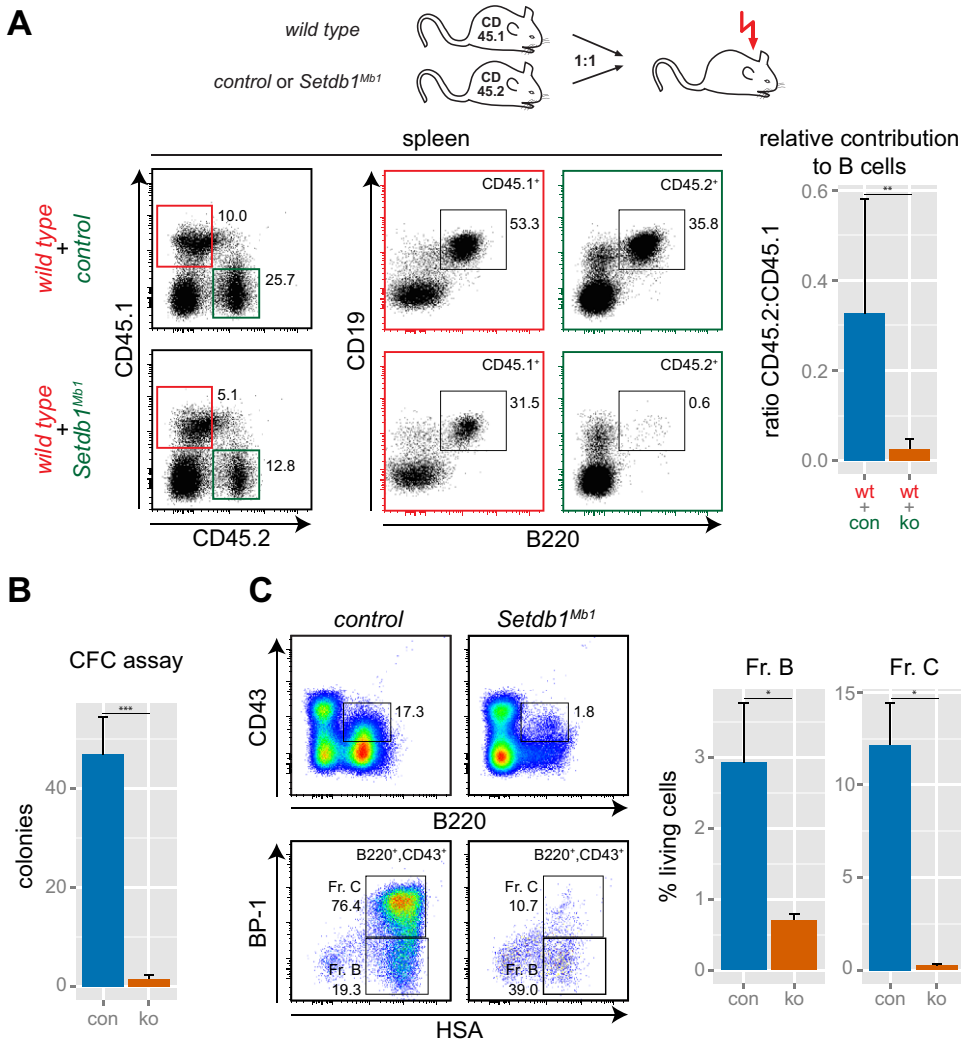


Fig. 2. *Setdb1* has cell-intrinsic functions in B cell development. (A) The bone marrow transplantation strategy (top). Representative FACS plots showing the relative contribution to the B cell lineage of wild-type versus control or *Setdb1^{Mb1}* donor bone marrow. The bar chart shows the quantification ($n=3$) of splenic B-cells (B220⁺ CD19⁺) in recipient mice as the ratio between control (con) or *Setdb1^{Mb1}* (ko) and wild type (wt). (B) Colony formation assay in MethoCult M3630 to support B-cell colony formation. Shown is the average colony number of three independent experiments with control and *Setdb1^{Mb1}* bone marrow cells ($n=3$). (C) Representative FACS analysis of differentiated B cells (CD43⁺ B220⁺) after 8 days of OP9 co-culture in the presence of IL7. Bar chart shows quantification of three independent experiments for HardyFr. B (B220⁺ CD43⁺ HSA⁺ BP-1⁻) and Fr. C (B220⁺ CD43⁺ HSA⁺ BP-1⁺) B cells. (A-C) * $P<0.05$, ** $P<0.01$, *** $P<0.001$ (unpaired two-tailed Student's t -test).

We then performed *in vitro* B cell differentiation assays. Control bone marrow cells readily formed colonies in IL7-supplemented MethoCult M3630 medium, which supports B cell differentiation. Conversely, almost no colonies were obtained from *Setdb1^{Mb1}* bone marrow (Fig. 2B). Furthermore, *in vitro* differentiation of lineage-depleted bone marrow cells on OP9 stromal cells in the presence of IL7 revealed severely impaired differentiation of *Setdb1^{Mb1}* progenitors into the B cell lineage (Fig. 2C). Thus, our data demonstrate an essential cell-autonomous function of *Setdb1* in the early stages of B cell development.

Transcriptional changes in *Setdb1^{Mb1}* pro-B cells

To identify the molecular mechanisms leading to impaired B cell development in the absence of *Setdb1*, we performed transcriptional profiling by high-throughput RNA sequencing (RNA-seq). RNA was isolated from FACS-sorted pro-B cells (CD19⁺ IgM⁻ IgD⁻ CD25⁻ Kit⁺) from control and *Setdb1^{Mb1}* mice. *Setdb1* was completely deleted in *Setdb1^{Mb1}* pro-B cells as no band could be detected upon PCR amplification of the floxed exon 4 (Fig. 3B). Through RNA-seq analysis we found 130 upregulated and 136 downregulated (>2-fold) genes in *Setdb1^{Mb1}* pro-B cells (Fig. 3A, Table S1). GO term analysis of the regulated genes revealed enrichment for pathways implicated in immune system development (Fig. 3C). However, closer examination of the dataset indicated that none of the known essential factors for B cell development was dysregulated.

Rather, we found transcriptional changes in genes associated with the pro-B to pre-B cell transition. One example is *Aiolos* (*Irf3*), which is normally upregulated in late pro-B cells. *Aiolos* expression was detected in control pro-B cells, but it failed to be activated in *Setdb1^{Mb1}* pro-B cells. This suggested that the pro-B cell population isolated from *Setdb1^{Mb1}* bone marrow resided in a more immature stage. To substantiate this finding we performed gene set enrichment analysis using gene sets that are representative of early pro-B and late pro-B/early pre-B cells, respectively (Jojic et al., 2013). Notably, the early pro-B signature was enriched in *Setdb1^{Mb1}* pro-B cells, whereas the late pro-B/early pre-B signature was over-represented in control cells (Fig. 3D). These analyses suggest a bias toward having reduced numbers of late pro-B/early pre-B cells in *Setdb1^{Mb1}* bone marrow. In order to test this hypothesis we analyzed B cell populations using a different marker set (Hardy et al., 1991). We found significantly reduced late pro-B/early pre-B cells [B220⁺ CD43 (Spn)⁺ HSA (CD24a)⁺ BP-1 (Enpep)^{+/−}] in *Setdb1^{Mb1}* mice (Fig. S3). These data suggest that the majority of the transcriptional changes that we detected by RNA-seq simply reflect the block in pro-B to pre-B cell transition in *Setdb1^{Mb1}* mice.

Setdb1 directly regulates retrotransposons

To identify genomic regions that may be controlled by *Setdb1* in pro-B cells, we performed chromatin immunoprecipitation for

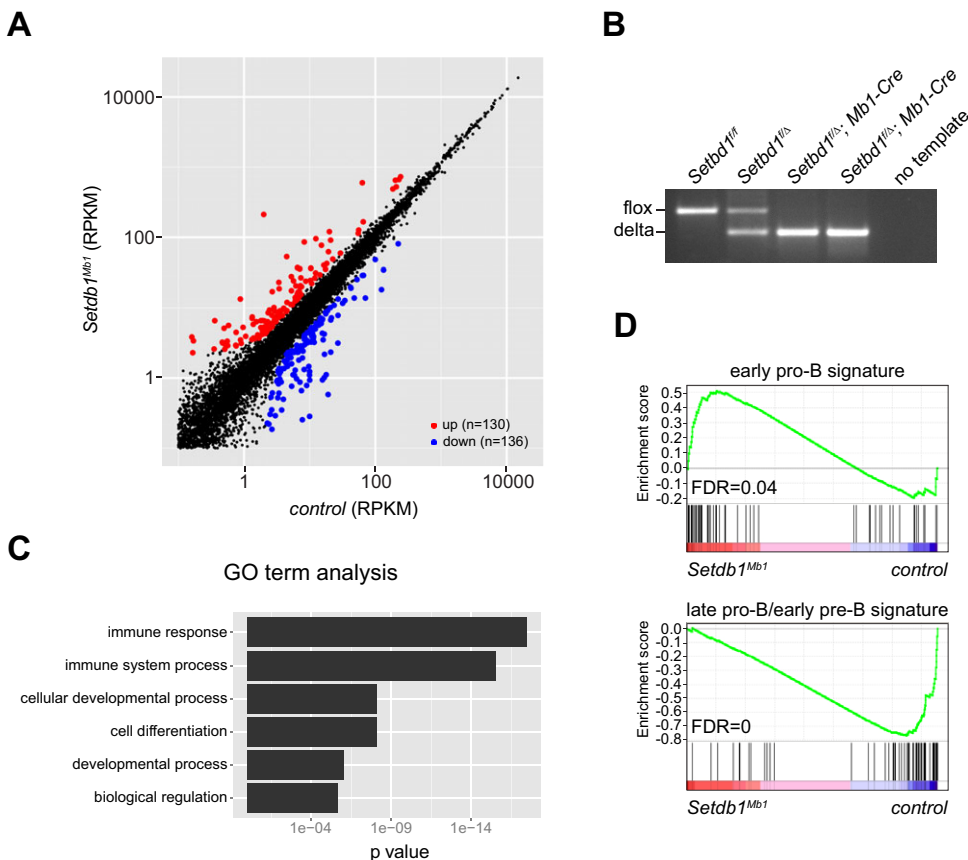


Fig. 3. Transcriptome analysis of *Setdb1*^{Mb1} pro-B cells reveals impaired pro-B to pre-B cell transition. (A) RNA-seq analysis performed on sorted control and *Setdb1*^{Mb1} pro-B cells (CD19⁺ IgD⁻ IgM⁻ Kit⁺ CD25⁻). Correlation plot shows expression levels of all genes in control and *Setdb1*-deficient pro-B cells as normalized RNA-seq read coverage in reads per kilobase per million reads (RPKM). Red dots, upregulated genes; blue dots, downregulated genes; black dots, genes with a less than 2-fold change in expression. (B) Deletion efficiency of the floxed *Setdb1* allele in pro-B cells as determined by PCR on genomic DNA. In *Setdb1*^{Mb1} (*Mb1-Cre*; *Setdb1*^{loxP}) pro-B cells, absence of the flox band indicates complete deletion of the floxed exon 4. (C) GO term enrichment analysis of the dysregulated genes in *Setdb1*^{Mb1} pro-B cells was performed with GStat (Beissbarth and Speed, 2004). *P*-values of the most highly enriched terms are plotted. (D) Gene set enrichment analysis of RNA-seq data from control and *Setdb1*^{Mb1} pro-B cells with gene lists representing Hardy Fr. A (B220⁺ CD43⁺ HSA^{low} BP-1⁻) and Fr. B/C (B220⁺ CD43⁺ HSA^{high}). *Setdb1*^{Mb1} pro-B cells displayed a clear enrichment for the Fr. A signature, whereas Fr. B/C signatures were depleted. FDR, false discovery rate.

Setdb1, H3K9me3 and H3K9ac in short-term cultured *Rag2*^{-/-} pro-B cells followed by high-throughput sequencing (ChIP-seq). This analysis revealed 5368 *Setdb1* binding sites in pro-B cells, which are shared in two independent datasets (see Fig. S4 for analysis of the individual datasets).

To determine the binding sites at which *Setdb1* could induce H3K9me3, we calculated the ChIP-seq read coverage for *Setdb1*, H3K9me3 and H3K9ac in 1500 bp windows across all *Setdb1* binding sites. These data were then clustered according to H3K9me3 and H3K9ac density (Fig. 4A). This analysis revealed that only a subset of *Setdb1* binding sites associates with H3K9me3 (clusters A, B). A large number of *Setdb1* peaks are found together with H3K9ac (clusters D, E, F) or do not display prominent enrichment for either H3K9me3 or H3K9ac (clusters C, G). We then analyzed the structural features underlying *Setdb1* binding sites. H3K9me3-associated regions are clearly enriched for repeat elements (clusters A, B). By contrast, H3K9ac-rich *Setdb1* peaks are mainly present at promoter regions (clusters D, E, F). We then asked whether genes near to *Setdb1* binding sites are transcriptionally regulated in *Setdb1*^{Mb1} pro-B cells. For each cluster, genes with a transcriptional start site within 5 kb of the *Setdb1* binding site were extracted. However, we could not detect any significant enrichment of regulated genes in any of the *Setdb1* binding site clusters. These data demonstrate that in pro-B cells *Setdb1* regulates only a small number of genes in the vicinity of its binding sites.

The ChIP-seq analysis showed that *Setdb1* binding sites that are enriched for H3K9me3 (clusters A, B) mainly reside within repeat elements. Therefore, we investigated whether distinct classes of repeat elements are dysregulated in *Setdb1*^{Mb1} pro-B cells. Analysis of our RNA-seq data uncovered three classes of retrotransposons

(MLV, MMVL30 and MMTV) to be upregulated in *Setdb1*^{Mb1} pro-B cells (Table S2, Fig. S5A). Re-examination of RNA-seq reads with unique mapping in the genome allowed to distinguish individual copies of these retrotransposon classes. The most strongly upregulated retrotransposons were four copies of the MLV class, with >100-fold overexpression (Fig. 4B). Notably, these four copies showed the strongest enrichment for *Setdb1* and H3K9me3 (Fig. 4C). Intriguingly, IAP-Ez retrotransposons, which are major targets of *Setdb1* in ESCs, were also enriched for *Setdb1* and H3K9me3 in pro-B cells, but did not show significantly enhanced expression in *Setdb1*^{Mb1} pro-B cells (Fig. 4B,C).

In summary, our data suggest that although *Setdb1* occupies many binding sites in pro-B cells, only a subset of these regions correlates with changes in gene expression when *Setdb1* is absent. Our results also show that in pro-B cells the major repressive function of *Setdb1* is exerted on specific classes of retrotransposons.

***Setdb1* mediates MLV silencing in pro-B cells**

Our ChIP-seq data revealed strongest enrichment of *Setdb1* and H3K9me3 at distinct MLV elements. Close inspection of the genomic regions around the depressed MLV retrotransposons revealed that genes in close proximity were also highly upregulated. An example is the MLV retrotransposon on chromosome 8 that lies in the vicinity of *Tubb3* and *Def8* (MLV8, Fig. 5A). *Tubb3* encodes a neuron-specific tubulin involved in axon guidance; *Def8* (differentially expressed in FDCP 8) is a largely uncharacterized gene of unknown function. RNA-seq data show strong derepression of MLV8 and upregulation of both *Tubb3* and *Def8*. Notably, upregulation of both genes is not mediated by read-through transcripts originating from MLV8, which is oriented tail-to-tail with *Tubb3* and head-to-head with *Def8*. ChIP-seq data revealed

enrichment of *Setdb1* and H3K9me3 across MLV8, but only background levels were detected across *Tubb3* and *Def8*. These data suggest that loss of *Setdb1* leads to derepression of MLV8, which then exerts enhancer effects on the neighboring genes leading to their upregulation. A similar example is MLV1, which lies in proximity to the *Fcgr2b* gene (Fig. S5B). In *Setdb1^{Mb1}* pro-B cells, both MLV1 and *Fcgr2b* are strongly derepressed (Fig. 5B) and *Fcgr2b* protein is even highly incorporated into the cell membrane (Fig. S5C,D). Interestingly, *Fcgr2b* is also upregulated in *Setdb1*-deficient T cells (Martin et al., 2015), although it remains to be determined if derepression of MLV1 can be observed in this context. RT-qPCR analyses for another MLV element (MLV5) similarly revealed strong derepression of the corresponding MLV transcript and upregulation of the neighboring gene (Fig. 5B).

To test whether *Setdb1*-dependent chromatin changes lead to dysregulation of MLV elements, we isolated control and *Setdb1^{Mb1}* CD43⁺ CD19⁺ pro-B cells by FACS sorting and performed ChIP-qPCR analyses. H3K9me3 was prominently enriched on MLV elements; however, loss of *Setdb1* only resulted in a small reduction of this modification (Fig. 5C). It is possible that other histone methyltransferases, such as *Suv39h*, contribute to H3K9me3 establishment (Bulut-Karslioglu et al., 2014). H3K4me3, a mark of active chromatin, was strongly elevated on MLV elements and on the promoters of *Tubb3* and *Def8* in *Setdb1*-deficient pro-B cells (Fig. 5D). No enrichment of H3K4me3 could be detected on IAP-Ez elements, which showed no transcriptional changes in *Setdb1^{Mb1}* pro-B cells. We also tested whether any changes in DNA methylation might contribute to transcriptional activation of these MLV elements. Very high levels of DNA methylation were detected in the strongly upregulated MLV8, demonstrating that loss of DNA methylation is not required for transcriptional activation (Fig. 5E, Fig. S6). IAP elements and a transcriptionally unchanged MLV retrotransposon did not show any changes in DNA methylation

(Fig. 5E, Fig. S6). Our data suggest that the presence of *Setdb1* inhibits the binding and/or activity of specific transcription factors that would otherwise establish an active chromatin structure. Complete loss of H3K9me3 or DNA methylation is apparently not necessary to allow the establishment of H3K4me3 and productive transcription.

Setdb1^{Mb1} pro-B cells die through apoptosis

Our transcriptional profiling of *Setdb1^{Mb1}* pro-B cells did not reveal dysregulation of important B cell-related transcription factors, which could have explained a developmental block. Another possible explanation for impaired B cell development is that pro-B cells die from apoptosis. To test if apoptosis is elevated in *Setdb1^{Mb1}* pro-B cells we performed annexin V (annexin A5) staining on control and *Setdb1^{Mb1}* bone marrow cells. In control mice, ~30% of pro-B cells enter apoptosis, which is likely to be due to non-productive VDJ recombination. Interestingly, the apoptosis rate was strongly increased in *Setdb1^{Mb1}* pro-B cells (Fig. 6A).

If enhanced apoptosis of pro-B cells is a major reason why B cell development is blocked in *Setdb1^{Mb1}* mice then we would predict that introducing a pro-survival protein might compensate for *Setdb1* deficiency in B cell development. To test this hypothesis we introduced an allele that overexpresses anti-apoptotic *Bcl2* in all hematopoietic cells [*Vav-Bcl2* (Egle et al., 2004)] into *Setdb1^{Mb1}* (*Setdb1^{Mb1}; Bcl2*) or control (*Bcl2*) mice. Apoptosis in both *Bcl2* and *Setdb1^{Mb1}; Bcl2* pro-B cells was comparably low (Fig. 6B). We then examined B cell development in the bone marrow of *Setdb1^{Mb1}; Bcl2* mice. Compared with *Setdb1^{Mb1}* (Fig. 1F,G) there was an increase in the percentages of pre-B, immature B and mature B cells in the *Setdb1^{Mb1}; Bcl2* mice (Fig. S7). Significant numbers of *Setdb1*-deficient mature B cells were observed in the spleen of *Setdb1^{Mb1}; Bcl2* mice (Fig. 6C-E), which were virtually absent in *Setdb1^{Mb1}* mice (Fig. 1D,E). These results were further

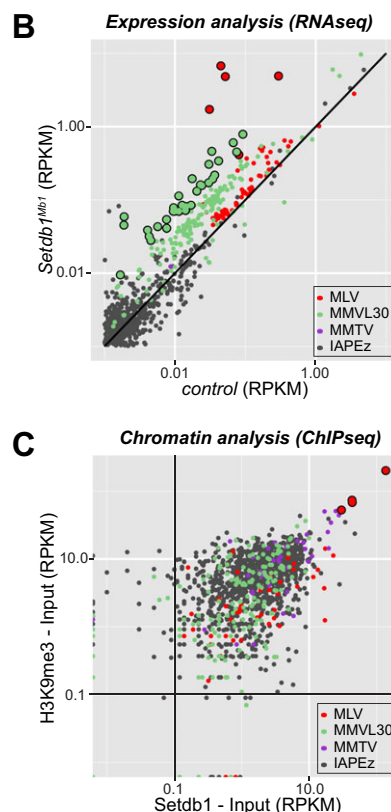
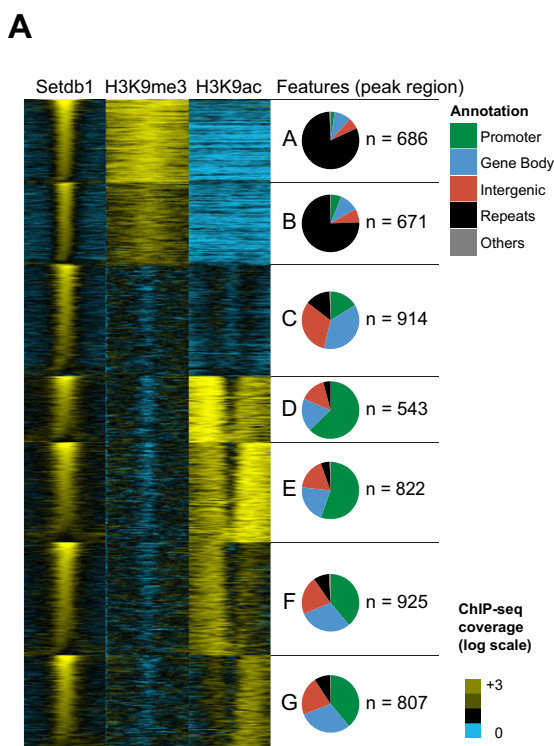


Fig. 4. *Setdb1* directly silences repetitive elements in pro-B cells. (A) ChIP-seq analysis for *Setdb1*, H3K9me3 and H3K9ac in short-term cultured *Rag2^{-/-}* pro-B cells. Heat map shows log-transformed read coverage for *Setdb1* and H3K9 modifications for 1500 bp across all *Setdb1* binding sites. Peak clusters were generated based on H3K9me3/H3K9ac occupancy using Cluster3 software. Pie charts depict the frequency of genomic features at *Setdb1* peaks in each cluster. (B) Double log scatter plot of normalized RNA-seq read coverage (RPKM) over distinct retrotransposon sequences in control and *Setdb1^{Mb1}* pro-B cells. Large dots depict retrotransposons with >5-fold expression changes. Strongest upregulation in *Setdb1^{Mb1}* pro-B cells was found for four MLV elements (large red dots). (C) Double log scatter plot of normalized ChIP-seq read coverage minus input (RPKM) for *Setdb1* and H3K9me3 over distinct retrotransposons. The four MLV retrotransposons with the highest expression changes (B) are again shown as large red dots.

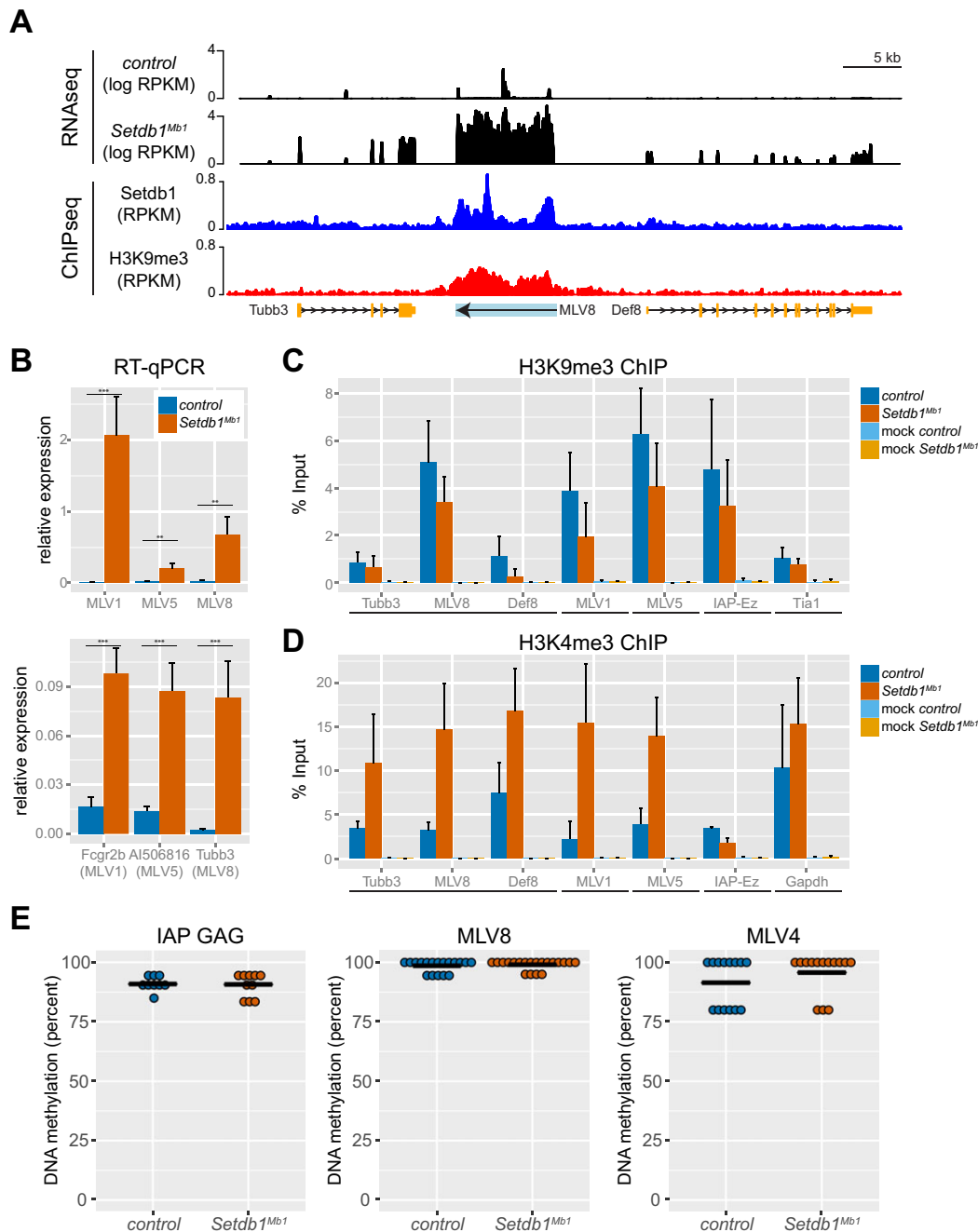


Fig. 5. *Setdb1* directly regulates MLV silencing by preventing establishment of active H3K4me3. (A) Coverage plot of normalized RNA-seq (control versus *Setdb1*^{Mb1} pro-B cells) and ChIP-seq (short-term cultured *Rag2*^{-/-} pro-B cells) coverage across the genomic region of MLV8. (B) RT-qPCR on the three most derepressed MLVs (top) and genes in their respective vicinity (bottom). Gene expression was calculated relative to housekeeping genes from six biological replicates. ***P*<0.01, ****P*<0.001 (unpaired two-tailed Student's *t*-test). (C) ChIP-qPCR (*n*=3) for H3K9me3 in control and *Setdb1*^{Mb1} pro-B cells on MLV retrotransposons and promoter regions of genes in their respective vicinity. IAP-Ez refers to the consensus primer set for IAP-Ez elements (positive control); Tia1 refers to the primer set for the promoter of the *Tia1* gene (negative control). (D) ChIP-qPCR (*n*=3) for H3K4me3 in control and *Setdb1*^{Mb1} pro-B cells on MLV retrotransposons and promoter regions of genes in their respective vicinity. IAP-Ez, consensus primer set for IAP-Ez elements (negative control); Gapdh, primer set for the promoter of the *Gapdh* gene (positive control). (E) DNA methylation of IAP GAG (no transcriptional change), MLV8 (derepressed) and MLV4 (no transcriptional change) was analyzed by bisulfite sequencing in control and *Setdb1*^{Mb1} pro-B cells. Plots show quantification of the DNA methylation analysis, with the bar indicating the mean.

supported by *in vitro* differentiation experiments with lineage-depleted bone marrow cells from *Bcl2* and *Setdb1*^{Mb1}; *Bcl2* mice, which showed almost comparable growth of pre-B cell colonies (Fig. 6F).

An important process during pro-B cell development is VDJ recombination of the *Igh* locus to produce a functional pre-B cell

receptor. Consistent with the block in pro-B to pre-B transition in *Setdb1*^{Mb1} mice, we detected lower efficiency of VDJ rearrangement (Fig. S8). By contrast, VDJ recombination was unaffected in *Setdb1*^{Mb1}; *Bcl2* pro-B cells (Fig. S8). Thus, our data demonstrate that counteracting apoptosis can partially rescue the developmental phenotype of *Setdb1*^{Mb1} mice.

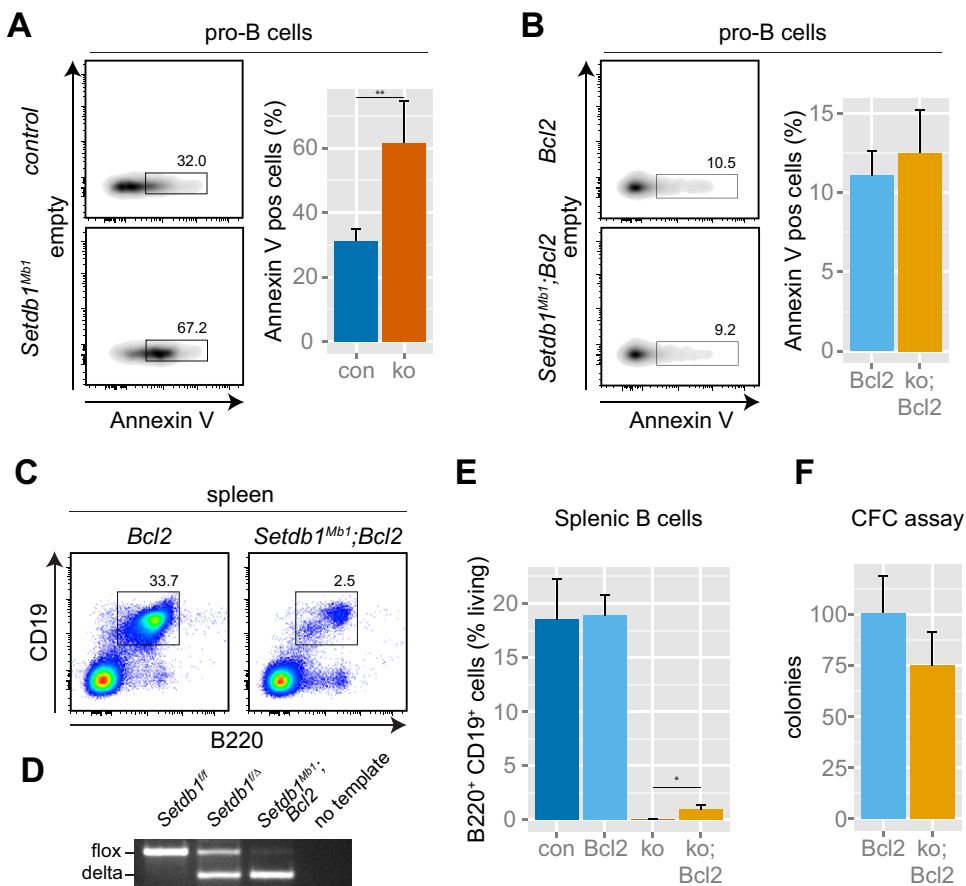


Fig. 6. *Setdb1^{Mdb1}* pro-B cells die from apoptosis. (A) Apoptosis in control and *Setdb1^{Mdb1}* pro-B cells (CD19⁺ IgM[−] IgD[−] CD25[−] Kit⁺) was measured by annexin V staining. Average percentages of annexin V-positive pro-B cells from six biological replicates are displayed in the bar chart. ***P*<0.01 (unpaired two-tailed Student's *t*-test). (B) Apoptosis in *Bcl2* and *Setdb1^{Mdb1}; Bcl2* pro-B cells (CD19⁺ IgM[−] IgD[−] CD25[−] Kit⁺) was measured by annexin V staining. Average percentages of annexin V-positive pro-B cells from six biological replicates are displayed in the bar chart. (C) Representative FACS analyses of splenic B cells (CD19⁺ B220⁺) in *Bcl2* and *Setdb1^{Mdb1}; Bcl2* mice. (D) *Setdb1* deletion rate monitored in sorted splenic B cells (IgM⁺ IgD⁺) by PCR. (E) Average percentages of splenic B cells from control, *Bcl2*, *Setdb1^{Mdb1}* and *Setdb1^{Mdb1}; Bcl2* mice (*n*=6). **P*<0.05 (unpaired two-tailed Student's *t*-test). (F) Colony formation assay in MethoCult M3630 for pre-B cell colony formation. Shown is the average colony number of three independent experiments with control (*Bcl2*) and *Setdb1^{Mdb1}; Bcl2* (ko; *Bcl2*) bone marrow cells.

Activation of the unfolded protein response pathway in *Setdb1^{Mdb1}* pro-B cells

We then examined whether apoptosis is linked with the transcriptional changes that we observe in *Setdb1^{Mdb1}* pro-B cells. As we only detected moderate regulation of protein-coding genes (Fig. 3), we hypothesized that upregulation of retrotransposons might lead to apoptosis. Upregulation of ERVs has been connected with enhanced DNA damage that may lead to apoptosis. However, we did not detect increased DNA breaks in *Setdb1^{Mdb1}* B cells (Fig. S9). We then attempted to establish whether the transcription of retrotransposons leads to the production of retroviral proteins. The top upregulated retrotransposon class in *Setdb1^{Mdb1}* pro-B cells is MLV. MLV transcripts have coding potential and can lead to the production of retroviral proteins. For example, the retroviral glycosylated envelope (Env) protein can be detected on cells with elevated expression of MLV transcripts (Evans et al., 1990; Young et al., 2012). We tested MLV Env protein production by FACS analysis and could detect high levels on the surface of *Setdb1^{Mdb1}* pro-B cells as compared with littermate controls (Fig. 7A). Western blot analyses confirmed high expression of MLV Env protein in *Setdb1*-deficient pro-B cells (Fig. S10A).

Could apoptosis in *Setdb1^{Mdb1}* pro-B cells be linked to the excessive production of MLV proteins? Unlike plasma cells, for example, which are specialized for the mass production of secreted proteins (Brewer and Hendershot, 2005; Gass et al., 2004), pro-B cells are relatively small, with a limited capacity to produce such proteins. The strongly elevated translation of proteins into the endoplasmic reticulum may lead to an accumulation of improperly folded proteins, which triggers a cellular stress pathway known as the unfolded protein response (UPR). We tested for activation of the

UPR pathway in *Setdb1^{Mdb1}* pro-B cells by expression analysis of key UPR genes.

A hallmark of the UPR response is the accumulation of a specific splice form of the mRNA encoding the transcription factor Xbp1 (Calton et al., 2002). Importantly, compared with control pro-B cells, we detected an increased level of spliced Xbp1 (Xbp1s) in *Setdb1*-deficient pro-B cells (Fig. 7B). Furthermore, expression of pro-apoptotic *Bcl2l11* was elevated (Fig. 7B). Other key UPR genes, such as those encoding the chaperones Hspa5 (Grp78 or BiP) and Pdia6 (Groenendyk et al., 2014; Lee, 2005), were also upregulated in *Setdb1*-deficient pro-B cells (Fig. 7B). As elevated apoptosis in *Setdb1^{Mdb1}* pro-B cells might prevent the accumulation of UPR transcripts, we also tested the UPR pathway in *Setdb1^{Mdb1}; Bcl2* pro-B cells. Notably, we detected even stronger upregulation of key UPR genes in *Setdb1^{Mdb1}; Bcl2* pro-B cells (Fig. 7B). In addition, gene set enrichment analysis using the hallmark gene sets from MySigDB revealed significant enrichment of the UPR gene signature in *Setdb1^{Mdb1}* pro-B cells (Fig. 7C). Thus, the increased expression of UPR components in both *Setdb1^{Mdb1}* and *Setdb1^{Mdb1}; Bcl2* pro-B cells clearly demonstrates activation of the UPR pathway.

The key inducer of apoptosis in the context of UPR is Bcl2l11 (Puthalakath et al., 2007). To test if apoptosis in *Setdb1^{Mdb1}* pro-B cells is mediated through Bcl2l11, we performed knockdown experiments in *in vitro* B cell differentiation assays. Control cells with scrambled shRNAs could readily form colonies in MethoCult M3630, whereas *Setdb1^{Mdb1}* cells did not form colonies (Fig. 7D). Knockdown of Bcl2l11 in *Setdb1^{Mdb1}* cells resulted in significantly elevated colony numbers (Fig. 7D), demonstrating that Bcl2l11 is mainly responsible for apoptosis induction in *Setdb1^{Mdb1}* cells.

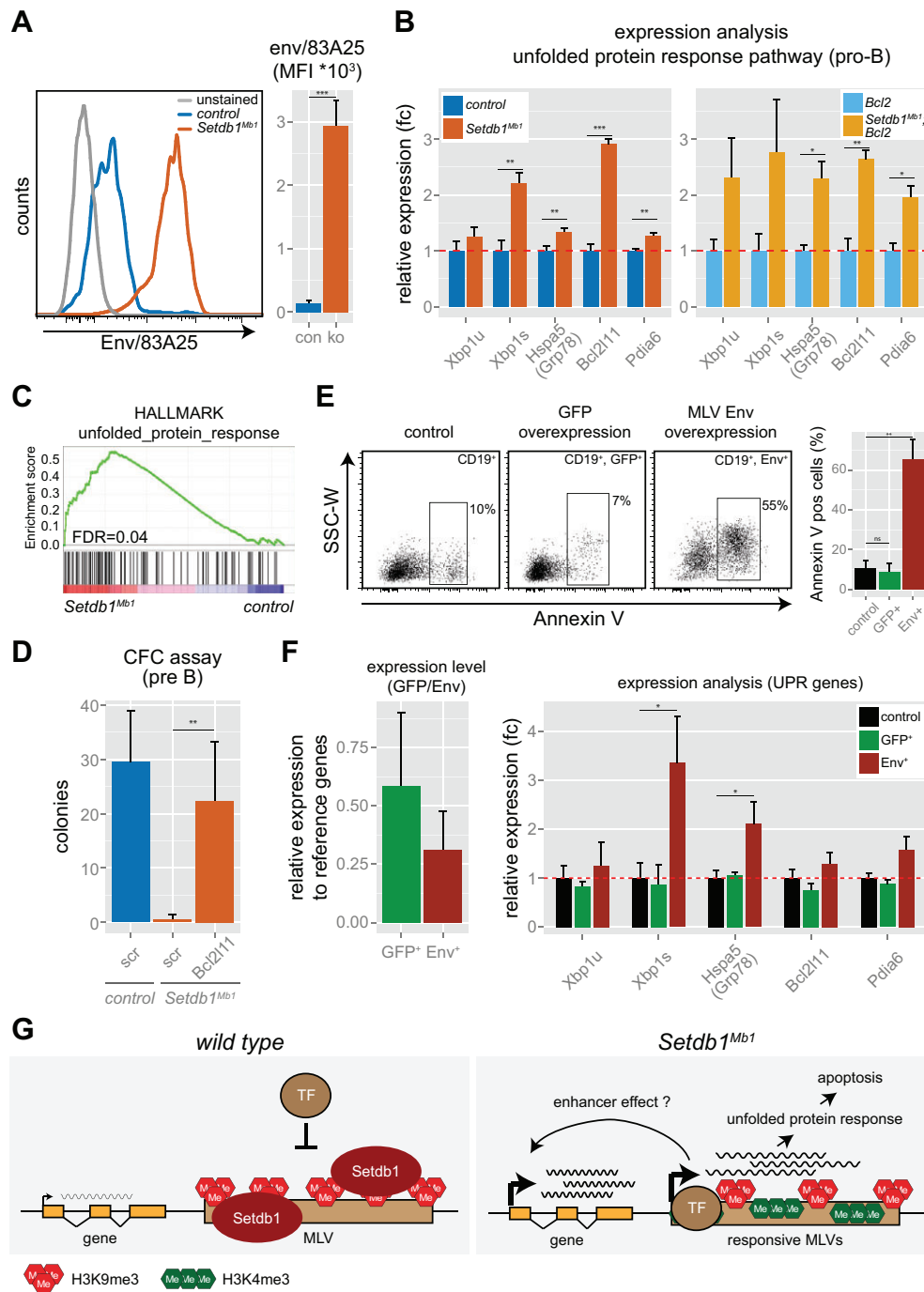


Fig. 7. Strong expression of MLV proteins leads to UPR-mediated apoptosis. (A) MLV envelope protein (Env) expression detected by FACS on control and *Setdb1*^{Mb1} pro-B cells (CD19⁺ IgM⁻ IgD⁻ Kit⁺). Bar chart depicts the average Env expression calculated as mean fluorescence intensity (MFI) from six mice per genotype. (B) RT-qPCR expression analyses of main UPR genes. Fold change (fc) gene expression of *Setdb1*^{Mb1} over control (left) and *Setdb1*^{Mb1}; *Bcl2* over *Bcl2* (right) pro-B cells (CD19⁺ IgM⁻ IgD⁻ CD25⁻ Kit⁺). *Xbp1u*, *Xbp1* normal splice form; *Xbp1s*, *Xbp1* UPR-related splice isoform; *Hspa5*, *Bcl2l11* and *Pdia6* are major mediators of the UPR response. (C) Gene set enrichment analysis of RNA-seq data from control and *Setdb1*^{Mb1} pro-B cells using the hallmark gene sets (MySigDB) reveals significant enrichment for the UPR gene set. (D) Colony formation assay in MethoCult M3630 for pre-B cell colony formation. The average colony number of three independent experiments with control and *Setdb1*^{Mb1} bone marrow cells infected with scrambled or *Bcl2l11*-specific shRNAs. (E) Overexpression of MLV Env protein induces apoptosis. Lineage-negative bone marrow cells (non-infected, GFP infected and MLV Env infected) were differentiated into B cells and apoptosis was measured by annexin V staining. (F) Overexpression of MLV Env protein induces UPR genes. (Left) RT-qPCR analysis of samples from E for expression levels of GFP and Env based on a common part of their transcripts. (Right) RT-qPCR expression analyses of main UPR genes in samples from E. Shown is the fold change in gene expression of GFP⁺ or Env⁺ B cells over non-transfected control cells. (A,B,D-F) **P*<0.05, ***P*<0.005, ****P*<0.001 (unpaired two-tailed Student's *t*-test); ns, not significant. (G) Model of the role of *Setdb1* in controlling the impact of retrotransposon expression on B cell development. In wild-type pro-B cells, *Setdb1* is recruited to retrotransposons and establishes H3K9me3. This presumably prevents access of transcription factors (TF) that have binding sites within the retrotransposon sequence. In *Setdb1*^{Mb1} pro-B cells, loss of *Setdb1* leads to the accumulation of H3K4me3 and strong transcription of retrotransposon sequences. MLV transcripts are translated and lead to the massive production of MLV envelope protein. This triggers activation of UPR and apoptosis of pro-B cells. Derepressed retrotransposons also act as enhancers and lead to the strong transactivation of genes in their vicinity.

Finally, we examined whether UPR-mediated apoptosis is mainly caused by overexpression of MLV proteins. We performed *in vitro* differentiation assays of wild-type cells in which we overexpressed GFP or MLV Env protein of the endogenous MLV1 retrovirus. Wild-type CD19⁺ B cells, in which we did not overexpress additional proteins, show a low rate of apoptosis (Fig. 7E). GFP overexpression in B cells did not reveal elevated apoptosis (Fig. 7E, Fig. S10B). By contrast, overexpression of MLV Env protein led to strongly increased apoptosis in B cells (Fig. 7E, Fig. S10B). Importantly, RT-qPCR analyses of *in vitro* differentiated B cells revealed specific activation of UPR genes upon Env overexpression (Fig. 7F).

In summary, our data show that elevated expression of MLV transcripts leads to excessive production of MLV Env protein, which triggers the UPR pathway, leading to apoptosis in *Setdb1*^{Mb1} pro-B cells and resulting in a block to B cell development.

DISCUSSION

Our study demonstrates that it is crucial to silence specific retrotransposons during development (Fig. 7G), which is in full agreement with a recent study of *Setdb1* function in B cells (Collins et al., 2015). In wild-type cells, *Setdb1* binds to MLV retrotransposons and establishes a repressive chromatin structure that prevents access of activating transcription factors. Upon deletion of *Setdb1* in pro-B cells, some ‘responsive’ MLV elements display strong transcriptional activity. It is possible that, owing to the loss of *Setdb1*, transcription factors can now access these MLVs leading to the establishment of active H3K4me3 marks. Interestingly, this activation can occur even though H3K9me3 is only minimally reduced and DNA methylation is unchanged. The activation of MLVs leads to two outcomes. First, responsive MLV retrotransposons may act as enhancers to strongly stimulate the transcription of neighboring genes. Second, the excessive production of MLV-derived proteins triggers UPR in pro-B cells, leading to apoptosis.

Genome-wide *Setdb1* binding had so far only been characterized in ESCs, where targets include retrotransposons and promoters of developmental genes (Bilodeau et al., 2009; Yuan et al., 2009). In pro-B cells, we also detected *Setdb1* on promoter regions; however, we did not observe strong transcriptional changes of these target genes in *Setdb1*-deficient pro-B cells. Interestingly, in pro-B cells, *Setdb1* is mostly unable to establish repressive H3K9me3 marks on promoter binding sites, as we detected strong H3K9ac occupancy at these regions. Transcription of these targets does not seem to be affected by *Setdb1* loss and, therefore, it is currently unclear what function *Setdb1* exerts on such binding sites. The major target sites at which *Setdb1* mediates establishment of H3K9me3 and transcriptional repression in pro-B cells are retrotransposons (Fig. 4). How *Setdb1* is recruited to these elements remains to be clarified. In ESCs, targeting is mainly mediated by Trim28; however, Trim28 is not enriched on MLV retrotransposons in B cells (Santoni de Sio et al., 2012). Moreover, Trim28 deletion in the B cell lineage did not result in impaired B cell development, but rather led to transcriptional dysregulation in mature B cells (Santoni de Sio et al., 2012). Thus, Trim28-dependent mechanisms are unlikely to mediate *Setdb1* targeting to MLVs.

Derepression of retrotransposons in *Setdb1*^{Mb1} pro-B cells implies that the absence of *Setdb1* allows binding of specific transcription factors to these elements. There is emerging evidence that transposable elements contain transcription factor binding sites (Xie et al., 2010) and may even physiologically act as tissue-specific enhancers (Xie et al., 2013). A recent study showed that the master

B cell transcription factor Pax5 may mediate forced expression of the same MLV elements that we found to be upregulated in *Setdb1*-deficient pro-B cells (Collins et al., 2015) (Table S3). However, additional cell type-specific transcription factors are likely to contribute to MLV transcription, as *Setdb1*-deficient mouse embryonic fibroblasts (Matsui et al., 2010) or myeloid cells (data not shown), which do not express Pax5, also display derepression of MLV retrotransposons. It is interesting to note that in pro-B cells only very few retrotransposon classes are derepressed, whereas *Setdb1*-deficient ESCs show strong derepression of many retrotransposon classes, including IAP-Ez, ETn, MusD and others (Karimi et al., 2011). In particular, in ESCs the major *Setdb1* targets are IAP-Ez elements, which, although bound by *Setdb1* and enriched for H3K9me3, display no transcriptional changes in *Setdb1*^{Mb1} pro-B cells. This might be explained by the lack of IAP-specific transcription factors in pro-B cells. Alternatively, redundant repression mechanisms, such as DNA methylation, might ensure silencing of these repeats in the absence of *Setdb1*. Consistent with this hypothesis, we did not detect significant changes in DNA methylation at these elements (Fig. 5).

Our data demonstrate that transcripts from endogenous MLV retroviruses have coding potential and lead to the strong production of MLV proteins. In pro-B cells, this triggers activation of the UPR pathway, and cells enter apoptosis. To our knowledge, this is the first demonstration that retrotransposon activation is linked with this specific cellular stress pathway. Several lines of evidence support our notion that UPR-mediated apoptosis is a major cause of impaired B cell development in *Setdb1*^{Mb1} mice. First, no crucial B cell transcription factors are dysregulated in *Setdb1*^{Mb1} pro-B cells (Fig. 3, Table S1). The only hematopoiesis-related gene that shows strong upregulation is *Fcgr2b* (Fig. S5). However, overexpression of *Fcgr2b* does not lead to defective B cell development (Brownlie et al., 2008). Second, the apoptosis phenotype is mainly due to elevated MLV protein expression, as overexpression of MLV Env protein is sufficient to induce apoptosis in B cells (Fig. 6D). Interestingly, expression of MLV Env protein from exogenous MLV retroviruses also results in increased apoptosis (Zhao and Yoshimura, 2008) and infection with MLV retroviruses results in impaired B cell development *in vivo* (Finstad et al., 2007). Furthermore, it is possible that transcripts/proteins produced from other upregulated repeat elements contribute to the phenotype. Third, blocking apoptotic pathways in *Setdb1*^{Mb1}; *Bcl2* mice resulted in a partial rescue of B cell development. Importantly, detection of mature B cells in the spleen of *Setdb1*^{Mb1}; *Bcl2* mice demonstrates that expression of key developmental genes is unlikely to be affected by *Setdb1*. The rescue might be partial because preventing apoptosis by *Bcl2* expression does not cease MLV Env production in *Setdb1*^{Mb1}; *Bcl2* pro-B cells. Therefore, those B cells are still compromised and may die through apoptosis-independent pathways. Lastly, apoptosis is mainly due to activation of the UPR pathway. We detect upregulation of key UPR genes in both *Setdb1*^{Mb1} and *Setdb1*^{Mb1}; *Bcl2* pro-B cells (Fig. 6B). Knockdown of the key UPR apoptosis inducer *Bcl2l1* leads to rescue of B cell development (Fig. 6C). We also attempted rescue experiments by knocking down other UPR components. However, owing to the redundancy in UPR signaling pathways, knockdown of individual UPR genes does not compromise UPR activation (Puthalakath et al., 2007). Furthermore, important UPR genes are essential for B cell development (Zhang et al., 2005) and cannot be knocked down. We cannot fully exclude additional causes for apoptosis, such as DNA damage or large-scale changes in chromatin architecture. However, as overexpression of MLV Env protein is already sufficient to

induce apoptosis (Fig. 6D) and to trigger UPR (Zhao and Yoshimura, 2008), our data strongly suggest that UPR activation is a major cause for apoptosis in *Setdb1^{Mb1}* pro-B cells. Unfortunately, owing to the limited number of pro-B cells and the unavailability of good antibodies, protein expression levels of UPR-related genes and protein-protein interactions between MLV-derived and UPR proteins could not be further assessed.

UPR-induced cell death mediated by retrotransposons might not be limited to pro-B cells. Derepression of other retrotransposon classes in different cell types may involve similar mechanisms. For example, apoptosis in *Setdb1*-deficient ESCs (Matsui et al., 2010) or neurons (Tan et al., 2012), which involve strong derepression of IAP retrotransposons, may be linked with UPR stress. However, additional cellular stress pathways exist that may detect the overexpression of endogenous retroviruses (ERVs) in other systems. For example, production of double-stranded RNA from ERVs could be recognized by specific pattern-recognition receptors leading to activation of the interferon response pathway (Roulois et al., 2015). Future experiments will reveal which cell types are particularly sensitive to overexpression of ERVs and which cellular pathway(s) can be triggered by distinct ERV classes.

MATERIALS AND METHODS

Mice and cell lines

Mice carrying the floxed *Setdb1* allele were purchased from the EUCOMM project [*Setdb1^{tm1a(EUCOMM)Wisi}*]. *Mb1-Cre* and *Vav-Bcl2* transgenes have been described previously (Egle et al., 2004; Hobeika et al., 2006). *Setdb1* genotyping is described in the supplementary Materials and Methods. Animals were housed in ventilated cages in the mouse facility at the Adolf Butenandt Institute. All procedures involving animals were in accordance with EU regulations. For the experiments, 5- to 10-week-old animals were used.

HEK 293T, OP9 stroma cells and progenitor cells were cultivated in DMEM (Gibco), IMDM and RPMI (Gibco), respectively. Media were supplemented with 10% FCS, 1% non-essential amino acids, 1% penicillin/streptomycin and 0.2% β -mercaptoethanol (Sigma). For progenitor cell short-term culture, RPMI was supplemented with 10 ng/ml IL7 (PeproTech).

Flow cytometry and cell sorting

Single-cell suspensions from bone marrow and spleen were stained for 20 min at 4°C using combinations of antibodies (see Table S4) conjugated with fluorochromes detectable in the following channels: FITC, PE, PE-Cy5, PE-Cy7, APC, APC-Cy7. All samples were pre-incubated for 20 min at 4°C with unconjugated CD16/CD32 (Fc γ 3) Fc-blocking antibody to avoid nonspecific binding, unless otherwise indicated. Data were acquired using a FACSCanto (BD Biosciences) and cell sorting was performed using either a MoFlo (Beckman Coulter) or FACSARIA III (BD Biosciences). Sorted samples were pretreated with red blood cell lysis buffer (BD Biosciences) or enriched using CD45R (B220) microbeads (Miltenyi). Data from flow cytometry were analyzed using FlowJo software (TreeStar).

Red blood cell lysis

Erythrocyte lysis was performed using BD Pharm Lyse (BD Pharmingen). 10 \times RBC lysis buffer (BD Biosciences) was diluted using distilled water and kept at room temperature. 3 ml 1 \times RBC lysis buffer was used to treat bone marrow cells derived from one mouse. Bone marrow cells were washed with 1 \times PBS and centrifuged at room temperature for 10 min at 1300 rpm (300 g). Pellets were incubated for 15 min at room temperature with 3 ml lysis buffer and then centrifuged at room temperature for 10 min at 1300 rpm. Cell pellets were then washed with 1 \times PBS to remove traces of lysis buffer and broken erythrocytes.

Definition of hematopoietic cell types for FACS analysis and FACS sorting

Hematopoietic cell types were defined according to specific surface markers, as detailed in the supplementary Materials and Methods and Table S5.

Bone marrow transplantation

Bone marrow cells were harvested from CD45.1 wild-type and CD45.2 donor mice 3–4 days after 5-fluorouracil (5-FU; Sigma) injection. To perform competitive bone marrow transplantation, 1 \times 10⁶ cells from CD45.1 wild-type mice were mixed 1:1 with cells from either control (*Mb1-Cre*;+/+) or *Mb1-Cre*; *Setdb1^{fllox/-}* (*Setdb1^{Mb1}*) mice. The mixture was transplanted into lethally irradiated (9 Gy) wild-type mice through tail vein injection. CD45.1 and CD45.2 surface markers were used to discriminate between the donors. Bone marrow and spleen from recipients were analyzed by flow cytometry 7 to 9 weeks after transplantation.

Histological analysis

Spleen from 6- to 8-week-old animals was fixed overnight in 4% formaldehyde and embedded in paraffin. Spleen sections were then stained with Hematoxylin and Eosin.

B cell colony formation assay and B cell differentiation on OP9 cells

To test B cell differentiation, lineage-depleted or whole bone marrow cells were treated with RBC lysis buffer and were seeded (1 \times 10⁵ cells/ml) in duplicate in 60 mm dishes on MethoCult M3630 (STEMCELL Technologies) containing IL7 according to the manufacturer's protocol. Cells were grown at 37°C in 5% CO₂ and checked each day to monitor colony formation. After 10–12 days of culture, colonies were scored and subsequently analyzed by flow cytometry using B220 and CD19 markers in combination with the viability dye 7AAD (eBioscience).

For short-term culture of B cell progenitors, lineage-negative bone marrow cells were enriched via magnetic sorting using the Lineage Cell Depletion Kit (Miltenyi). 5 \times 10⁵ to 1 \times 10⁶ cells were seeded in 24-well plates together with OP9 stromal cell in the presence of IL7 (10 ng/ml). Every other day, cells were split onto a fresh OP9 cell layer with IL7-supplemented medium as previously described (Holmes and Zuniga-Pflucker, 2009). At day 10 of co-culture, cells were harvested and analyzed by flow cytometry for pre-B cell differentiation using the Hardy scheme (Hardy et al., 1991).

Annexin V staining

Annexin V staining was performed using the Annexin V Apoptosis Detection Kit (eBioscience). 1–2 \times 10⁶ bone marrow cells were prestained for pro-B cell markers. Next, cells were stained with annexin V according to the kit protocol. To remove unbound annexin V, cells were washed with 1–2 ml annexin V buffer and immediately analyzed by FACS.

VDJ recombination

Genomic DNA from FACS-sorted bone marrow cells was analyzed for VDJ recombination as described in the supplementary Materials and Methods.

DNA methylation analysis

Genomic DNA from control and *Setdb1^{Mb1}* pro-B cells was subjected to bisulfite conversion and sequencing as described in the supplementary Materials and Methods and Table S6.

DNA damage analysis

γ H2A.X foci were enumerated in bone marrow cells as described in the supplementary Materials and Methods.

Expression analysis by RT-qPCR

Pro-B cells were sorted with either MoFlo or FACSARIA III. For gene expression analyses in *Setdb1^{Mb1}* pro-B cells, RNA was isolated using the RNeasy Plus Kit (Qiagen). Genomic DNA retained by the gDNA columns was purified and used to test the *Setdb1* deletion rate.

Alternatively, to detect gene expression changes in *Setdb1^{Mb1}*; *Bcl2* pro-B cells, mRNA was isolated using Trizol or Direct-zol RNA MiniPrep (Zymo Research). To remove genomic DNA contamination, samples were treated with DNase I (Roche). cDNA was synthesized using random hexamer primers. Ct values were obtained by performing qPCR using SYBR Green dye. Differences in gene expression were calculated either as

fold change using the $2^{-\Delta\Delta CT}$ algorithm or as relative expression to housekeeping genes.

RNA-seq

Pro-B cells were sorted using MoFlo and RNA was isolated using the RNeasy Plus Kit (Qiagen). Library preparation was performed as previously described (Schwickert et al., 2014). For further details, see the supplementary Materials and Methods.

ChIP-seq and ChIP-qPCR

Short-term cultured *Rag2*^{-/-} pro-B cells were obtained *in vitro* by cultivating them together with OP9 stromal cells in the presence of IL7. After 5-6 days of expansion, CD19⁺ B cells were enriched by magnetic sorting and processed to precipitate chromatin using antibodies against Setdb1, H3K9me3 and H3K9ac according to Schwickert et al. (2014). For further details, see the supplementary Materials and Methods, Tables S4 and S7.

Statistical analysis

Statistical differences between control and mutant groups were determined by unpaired or paired *t*-tests. *P*<0.05 was considered significant. Graphs were prepared and statistical tests were performed using R. Bar charts show mean values; error bars denote s.d.

shRNA knockdown and MLV overexpression in B cells

The coding sequence of the envelope protein encoded by MLV1 was PCR amplified using primer pair (5'-3') ATGGAAGGTCCAGCGTTCT and ACCAAGAACAACCCAGCT. The amplicon was gel purified and used as template for a second amplification with primers ATGGAAGGTCCA-GCGTTCT and TTATTCACGCGATTCTACTTCT. The resulting fragment was cloned into pLenti6 vector. Detection of MLV Env protein is described in the supplementary Materials and Methods.

A validated *Bcl2l1l*-specific shRNA sequence (TRC shRNA library, Sigma Aldrich) was integrated into the pLKO1 vector using sequence 5'-CGCGTCCGGGACGAGTCAACGAAACTTACCT-CGAGGTAAGTTTCGTTGAACTCGTCTTTTGGAAATTAC-3'. The sequence of the scrambled shRNA is 5'-CGCGTCCGGCAACAAGATG-AAGAGCACCAACTCGAGTTGGTGCTCTTCATCTTGTGTTTTG-GAAA-3'.

For overexpression and shRNA knockdown, lentiviral particles were produced according to Sadic et al. (2015) and used to transduce 3-4×10⁵ hematopoietic progenitors (lineage negative) prestimulated for 2 days with IL7 (10 ng/ml). Progenitors transduced with viruses carrying shRNA were kept in culture for 24 h before seeding in MethoCult M3630 containing 0.5 µg/ml puromycin. For overexpression assays, transduced cells were kept in culture for 3 days in RPMI supplemented with IL7 (10 ng/ml) before FACS analysis.

For details of the associated lentiviral packaging, overexpression and shRNA plasmid constructs, see Table S8.

Acknowledgements

We thank Frank Malik for generously providing the 83A25 (Env) antibody and Marc Schmidt-Suppran for sharing the *Mb1-Cre* mice.

Competing interests

The authors declare no competing or financial interests.

Author contributions

G.S., A.P., A.E., G.P.d.A., L.K. and M.B. contributed to concepts and approaches; A.P., G.P.d.A., A.E., M.H., M.K., A.N. and J.E. performed experiments; A.P., A.E., G.P.d.A., M.K. and G.S. analyzed data; G.S. prepared the manuscript; A.P., A.E., G.P.d.A., L.K. and M.B. edited the manuscript.

Funding

Work in the G.S. laboratory was funded by the Deutsche Forschungsgemeinschaft [SFB684 A17 and SFB1064, A11]. L.K. was supported by the Deutsche Forschungsgemeinschaft. M.B. is supported by Boehringer Ingelheim and a European Research Council Advanced Grant [291740-LymphoControl] from the European Community's Seventh Framework Program. This work was also

supported by a Brazilian National Council for Scientific and Technological Development (CNPq-Brazil; Conselho Nacional de Desenvolvimento Científico e Tecnológico) fellowship to G.P.d.A. [process number 204724/2013-9].

Data availability

The ChIP-seq and RNA-seq data reported in this paper have been deposited at Gene Expression Omnibus with accession number GSE77636.

Supplementary information

Supplementary information available online at <http://dev.biologists.org/lookup/suppl/doi:10.1242/dev.130203/-/DC1>

References

- Beguelin, W., Popovic, R., Teater, M., Jiang, Y., Bunting, K. L., Rosen, M., Shen, H., Yang, S. N., Wang, L., Ezponda, T. et al. (2013). EZH2 is required for germinal center formation and somatic EZH2 mutations promote lymphoid transformation. *Cancer Cell* **23**, 677-692.
- Beissbarth, T. and Speed, T. P. (2004). Gostat: find statistically overrepresented Gene Ontologies within a group of genes. *Bioinformatics* **20**, 1464-1465.
- Bilodeau, S., Kagey, M. H., Frampton, G. M., Rahl, P. B. and Young, R. A. (2009). SetDB1 contributes to repression of genes encoding developmental regulators and maintenance of ES cell state. *Genes Dev.* **23**, 2484-2489.
- Bourc'his, D. and Bestor, T. H. (2004). Meiotic catastrophe and retrotransposon reactivation in male germ cells lacking Dnmt3L. *Nature* **431**, 96-99.
- Brewer, J. W. and Hendershot, L. M. (2005). Building an antibody factory: a job for the unfolded protein response. *Nat. Immunol.* **6**, 23-29.
- Brownlie, R. J., Lawlor, K. E., Niederer, H. A., Cutler, A. J., Xiang, Z., Clatworthy, M. R., Floto, R. A., Greaves, D. R., Lyons, P. A. and Smith, K. G. (2008). Distinct cell-specific control of autoimmunity and infection by FcγRIIIb. *J. Exp. Med.* **205**, 883-895.
- Bulut-Karslioglu, A., De La Rosa-Velazquez, I. A., Ramirez, F., Barenboim, M., Onishi-Seebacher, M., Arand, J., Galan, C., Winter, G. E., Engist, B., Gerle, B. et al. (2014). Suv39h-dependent H3K9me3 marks intact retrotransposons and silences LINE elements in mouse embryonic stem cells. *Mol. Cell* **55**, 277-290.
- Calfon, M., Zeng, H., Urano, F., Till, J. H., Hubbard, S. R., Harding, H. P., Clark, S. G. and Ron, D. (2002). IRE1 couples endoplasmic reticulum load to secretory capacity by processing the XBP-1 mRNA. *Nature* **415**, 92-96.
- Collins, P. L., Kyle, K. E., Egawa, T., Shinkai, Y. and Oltz, E. M. (2015). The histone methyltransferase SETDB1 represses endogenous and exogenous retroviruses in B lymphocytes. *Proc. Natl. Acad. Sci. USA* **112**, 8367-8372.
- Dodge, J. E., Kang, Y.-K., Beppu, H., Lei, H. and Li, E. (2004). Histone H3-K9 methyltransferase ESET is essential for early development. *Mol. Cell. Biol.* **24**, 2478-2486.
- Egle, A., Harris, A. W., Bath, M. L., O'Reilly, L. and Cory, S. (2004). VavP-Bcl2 transgenic mice develop follicular lymphoma preceded by germinal center hyperplasia. *Blood* **103**, 2276-2283.
- Evans, L. H., Morrison, R. P., Malik, F. G., Portis, J. and Britt, W. J. (1990). A neutralizable epitope common to the envelope glycoproteins of ecotropic, polytropic, xenotropic, and amphotropic murine leukemia viruses. *J. Virol.* **64**, 6176-6183.
- Finstad, S. L., Rosenberg, N. and Levy, L. S. (2007). Diminished potential for B-lymphoid differentiation after murine leukemia virus infection *in vivo* and in EML hematopoietic progenitor cells. *J. Virol.* **81**, 7274-7279.
- Gass, J. N., Gunn, K. E., Sriburi, R. and Brewer, J. W. (2004). Stressed-out B cells? Plasma-cell differentiation and the unfolded protein response. *Trends Immunol.* **25**, 17-24.
- Groenendyk, J., Peng, Z., Dudek, E., Fan, X., Mizianty, M. J., Dufey, E., Urna, H., Sepulveda, D., Rojas-Rivera, D., Lim, Y. et al. (2014). Interplay between the oxidoreductase PDIA6 and microRNA-322 controls the response to disrupted endoplasmic reticulum calcium homeostasis. *Sci. Signal.* **7**, ra54.
- Hardy, R. R., Carmack, C. E., Shinton, S. A., Kemp, J. D. and Hayakawa, K. (1991). Resolution and characterization of pro-B and pre-pro-B cell stages in normal mouse bone marrow. *J. Exp. Med.* **173**, 1213-1225.
- Heng, T. S. P., Painter, M. W. and The Immunological Genome Project Consortium. (2008). The Immunological Genome Project: networks of gene expression in immune cells. *Nat. Immunol.* **9**, 1091-1094.
- Hobeika, E., Thiemann, S., Storch, B., Jumaa, H., Nielsen, P. J., Pelanda, R. and Reth, M. (2006). Testing gene function early in the B cell lineage in mb1-cre mice. *Proc. Natl. Acad. Sci. USA* **103**, 13789-13794.
- Holmes, R. and Zuniga-Pflucker, J. C. (2009). The OP9-DL1 system: generation of T-lymphocytes from embryonic or hematopoietic stem cells *in vitro*. *Cold Spring Harb. Protoc.* **2009**, pdb.prot5156.
- Jojic, V., Shay, T., Sylvia, K., Zuk, O., Sun, X., Kang, J., Regev, A., Koller, D., The Immunological Genome Project Consortium, Best, A. J. et al. (2013). Identification of transcriptional regulators in the mouse immune system. *Nat. Immunol.* **14**, 633-643.
- Karimi, M. M., Goyal, P., Maksakova, I. A., Bilenky, M., Leung, D., Tang, J. X., Shinkai, Y., Mager, D. L., Jones, S., Hirst, M. et al. (2011). DNA methylation and

- SETDB1/H3K9me3 regulate predominantly distinct sets of genes, retroelements, and chimeric transcripts in mESCs. *Cell Stem Cell* **8**, 676-687.
- Lawson, K. A., Teteak, C. J., Gao, J., Li, N., Hacquebord, J., Ghatan, A., Zielinska-Kwiatkowska, A., Song, G., Chansky, H. A. and Yang, L. (2013). ESET histone methyltransferase regulates osteoblastic differentiation of mesenchymal stem cells during postnatal bone development. *FEBS Lett.* **587**, 3961-3967.
- Lee, A. S. (2005). The ER chaperone and signaling regulator GRP78/BiP as a monitor of endoplasmic reticulum stress. *Methods* **35**, 373-381.
- Lee, E., Iskow, R., Yang, L., Gokcumen, O., Haseley, P., Luquette, L. J., III, Lohr, J. G., Harris, C. C., Ding, L., Wilson, R. K. et al. (2012). Landscape of somatic retrotransposition in human cancers. *Science* **337**, 967-971.
- Martin, F. J., Xu, Y., Lohmann, F., Ciccone, D. N., Nicholson, T. B., Loureiro, J. J., Chen, T. and Huang, Q. (2015). KMT1E-mediated chromatin modifications at the FcgammaRIIb promoter regulate thymocyte development. *Genes Immun.* **16**, 162-169.
- Matsui, T., Leung, D., Miyashita, H., Maksakova, I. A., Miyachi, H., Kimura, H., Tachibana, M., Lorincz, M. C. and Shinkai, Y. (2010). Proviral silencing in embryonic stem cells requires the histone methyltransferase ESET. *Nature* **464**, 927-931.
- Puthalakath, H., O'Reilly, L. A., Gunn, P., Lee, L., Kelly, P. N., Huntington, N. D., Hughes, P. D., Michalak, E. M., McKimm-Breschkin, J., Motoyama, N. et al. (2007). ER stress triggers apoptosis by activating BH3-only protein Bim. *Cell* **129**, 1337-1349.
- Regha, K., Sloane, M. A., Huang, R., Pauley, F. M., Warczok, K. E., Melikant, B., Radolf, M., Martens, J. H. A., Schotta, G., Jenuwein, T. et al. (2007). Active and repressive chromatin are interspersed without spreading in an imprinted gene cluster in the mammalian genome. *Mol. Cell* **27**, 353-366.
- Roulois, D., Loo Yau, H., Singhanian, R., Wang, Y., Danesh, A., Shen, S. Y., Han, H., Liang, G., Jones, P. A., Pugh, T. J. et al. (2015). DNA-demethylating agents target colorectal cancer cells by inducing viral mimicry by endogenous transcripts. *Cell* **162**, 961-973.
- Sadic, D., Schmidt, K., Groh, S., Kondofersky, I., Ellwart, J., Fuchs, C., Theis, F. J. and Schotta, G. (2015). Atrx promotes heterochromatin formation at retrotransposons. *EMBO Rep.* **16**, 836-850.
- Santoni de Sio, F. R., Massacand, J., Barde, I., Offner, S., Corsinotti, A., Kapopoulou, A., Bojkowska, K., Dagklis, A., Fernandez, M., Ghia, P. et al. (2012). KAP1 regulates gene networks controlling mouse B-lymphoid cell differentiation and function. *Blood* **119**, 4675-4685.
- Schwickert, T. A., Tagoh, H., Gultekin, S., Dakic, A., Axelsson, E., Minnich, M., Ebert, A., Werner, B., Roth, M., Cimmino, L. et al. (2014). Stage-specific control of early B cell development by the transcription factor Ikaros. *Nat. Immunol.* **15**, 283-293.
- Su, I.-H., Basavaraj, A., Krutchinsky, A. N., Hobert, O., Ullrich, A., Chait, B. T. and Tarakhovskiy, A. (2003). Ezh2 controls B cell development through histone H3 methylation and Igh rearrangement. *Nat. Immunol.* **4**, 124-131.
- Tan, S.-L., Nishi, M., Ohtsuka, T., Matsui, T., Takemoto, K., Kamio-Miura, A., Aburatani, H., Shinkai, Y. and Kageyama, R. (2012). Essential roles of the histone methyltransferase ESET in the epigenetic control of neural progenitor cells during development. *Development* **139**, 3806-3816.
- Xie, D., Chen, C.-C., Ptaszek, L. M., Xiao, S., Cao, X., Fang, F., Ng, H. H., Lewin, H. A., Cowan, C. and Zhong, S. (2010). Rewirable gene regulatory networks in the preimplantation embryonic development of three mammalian species. *Genome Res.* **20**, 804-815.
- Xie, M., Hong, C., Zhang, B., Lowdon, R. F., Xing, X., Li, D., Zhou, X., Lee, H. J., Maire, C. L., Ligon, K. L. et al. (2013). DNA hypomethylation within specific transposable element families associates with tissue-specific enhancer landscape. *Nat. Genet.* **45**, 836-841.
- Yang, L., Lawson, K. A., Teteak, C. J., Zou, J., Hacquebord, J., Patterson, D., Ghatan, A. C., Mei, Q., Zielinska-Kwiatkowska, A., Bain, S. D. et al. (2013). ESET histone methyltransferase is essential to hypertrophic differentiation of growth plate chondrocytes and formation of epiphyseal plates. *Dev. Biol.* **380**, 99-110.
- Young, G. R., Eksmond, U., Salcedo, R., Alexopoulou, L., Stoye, J. P. and Kassiotis, G. (2012). Resurrection of endogenous retroviruses in antibody-deficient mice. *Nature* **491**, 774-778.
- Yuan, P., Han, J., Guo, G., Orlov, Y. L., Huss, M., Loh, Y.-H., Yaw, L.-P., Robson, P., Lim, B. and Ng, H.-H. (2009). Eset partners with Oct4 to restrict extraembryonic trophoblast lineage potential in embryonic stem cells. *Genes Dev.* **23**, 2507-2520.
- Zhang, K., Wong, H. N., Song, B., Miller, C. N., Scheuner, D. and Kaufman, R. J. (2005). The unfolded protein response sensor IRE1alpha is required at 2 distinct steps in B cell lymphopoiesis. *J. Clin. Invest.* **115**, 268-281.
- Zhao, X. and Yoshimura, F. K. (2008). Expression of murine leukemia virus envelope protein is sufficient for the induction of apoptosis. *J. Virol.* **82**, 2586-2589.